

Fatigue Performance of Marine Composite Doubler Plate Joints under Random Load Spectra

By

Steven P. Blake
Roberto A. Lopez-Anido
Fadi W. El-Chiti
AEWC Center
Department of Civil and Environmental Engineering
University of Maine

Abstract

Composite structures commonly fail at secondary bonded joints due to crack propagation at the bond line of the joint. The crack propagation response of secondary bonded doubler plate joints in fiber-reinforced polymer (FRP) composite panels was investigated due to variable amplitude fatigue produced by vessel design spectra loads. The doubler plate joints were analyzed with respect to lifespan and failure criteria typically used for marine composites. The goal of the study is to characterize crack propagation in secondary bonded doubler plate joints under variable amplitude fatigue produced by design spectra loads for seaframes. The main contribution of the study to the marine industry is to improve current design methods for doubler plate joints in vessels under service conditions. Furthermore, the study serves to gain a better understanding of fatigue life prediction in secondary bonded joints for marine composites. The research method adopted in the study is to determine a fatigue load scale factor, which can be applied to the ultimate quasi-static strength of an FRP composite doubler plate joint. A test method was developed, and a modified Miner's Rule approximation was implemented in determining the damage at failure and estimating preliminary load scale factors. Two fatigue spectra were used to model the stress induced over a full 30-year life cycle of the doubler plate joints in seaframes. Preliminary results have yielded insight into how crack propagation in secondary bonded doubler plate joints progresses under variable amplitude fatigue.

Introduction

Composite materials are becoming increasingly used in large scale marine construction for structural purposes. As a result, more focus has been placed on failure prediction and service life design of various structural composite members and joints. Serviceability issues of marine composites include relaxation of stiffness and ultimate strength as well as crack propagation (1). Crack propagation is a common cause of failure in marine composites at joint locations. Various methods have been adopted to both predict and detect failure of composite members and joints (1), (2). However, there has been minimal testing done to determine the service life of a structural FRP component under actual loading conditions. Previous research has shown that the organization of stress levels within a particular fatigue spectrum can have great effect on the outcome of experimental results of FRP composites (2). Constant amplitude fatigue testing is commonly used to predict the service life of most structural materials; however, research has shown that constant amplitude fatigue testing is not adequate for service life prediction of FRP composites (2), (4). For the purpose of this paper, random block loading spectra were used. This paper deals primarily with crack propagation as a serviceability issue in secondary bonded doubler plate joints in FRP composite panels.

Objective - Approach

The goal of this study is to characterize crack propagation in secondary bonded doubler plate joints under variable amplitude service level fatigue loading with the specific objective of improving current design methods for this type of joint as well as to build upon current understanding of crack propagation in FRP composites due to fatigue loading. To address this objective a fatigue load scale factor was determined, which could then be applied to the ultimate quasi-static strength of an FRP composite doubler joint plate. Failure was considered to be 0.25 inch (6.4 mm) crack propagation between the primary and secondary bond surfaces, which is a commonly used criterion in the inspection of marine composite joints.

All testing was performed on specimens cut from a single secondary bonded FRP doubler joint plate. Testing was conducted to determine the quasi-static strength of the doubler joint plate under tensile loading, and a series of tension-tension fatigue tests with a minimum to maximum load ratio (R) of 0.1 was then conducted with various applied scale factors. The load ratio, R , of 0.1 was adopted based on values reported in the literature for fatigue tests performed on similar tapered composite specimens (6). Following each set of fatigue tests, a new scale factor was determined by back-calculating a theoretical failure damage using the Palmgren-Miner rule.

Miner's Rule

The earliest model used for predicting cumulative damage of composite materials under variable amplitude fatigue is the Palmgren-Miner rule:

$$D = \sum_{i=1}^k \frac{n_i}{N_i} \quad (1)$$

Where D is the cumulative damage, k is the number of applied load levels, n_i is the number of constant amplitude cycles at the i th load level, and N_i is the number of cycles to failure at the i th load level (5). Because of its simplicity and wide use, the Palmgren-Miner rule was used to estimate the scaled factor to be applied to the fatigue loading spectra.

Results from previous constant amplitude fatigue test data were used to plot the load level vs. the number of cycles to failure (S-N curve). Single amplitude fatigue peak loads from previous tests were normalized to width to account for specimen variability. Furthermore, the normalized fatigue peak loads were divided by the normalized ultimate static tensile strength. The normalized fatigue peak loads, which were defined between 0 and 1, were plotted against the number of cycles to failure, and the following logarithmic relationship was found, as shown in Figure 1:

$$SI_i = A * \ln(N_i) + B \quad (2)$$

Where SI is the normalized fatigue peak load or stress index at each load level, N is the number of cycles to failure, B is the equivalent of the normalized failure load at one cycle, and A is a constant determined experimentally. A curve fit was performed and B was forced to one, the average normalized ultimate tensile strength at one cycle is shown in Figure 2. For this experiment, the constant, A , was determined to be -0.061. Using this relationship the number of cycles to failure for a particular stress level could be estimated as shown:

$$e^{\left(\frac{SI_i - 1}{A}\right)} = N_i \quad (3)$$

Variable Amplitude Fatigue Spectra

Two fatigue loading spectra were used, an initial 5-year break-in spectrum followed by 25 1-year spectra. The purpose of using the two spectra was to simulate a target 30-year lifespan. Random block loading spectra were used to simulate the 30-year lifespan rather than equivalent damage constant amplitude spectra. Previous research has indicated that random fatigue loading can be more damaging to composite materials than constant amplitude fatigue loading. Several studies have been conducted characterizing the response of composites to variable amplitude fatigue. In these studies, either high amplitude cycling followed by low amplitude cycling or low amplitude cycling followed by high amplitude cycling were adopted. A review on the subject of load se-

quence effects conducted by Paepegem and Degrieck (4) concluded that there is little agreement as to what type of loading arrangement is the most conservative. Another study, conducted by Post (2) included coupon test results in direct tension and compression from three different spectra: High amplitude to low amplitude, low amplitude to high amplitude, and random cycling. The results from this study showed that random cycling produced the greatest number of premature failures and thus was the most conservative. Because of the similarity between the composite material and lay-up used by Post and that adopted in this study, random block loading spectra were used.

Each spectrum was normalized to the maximum amplitude as shown in Table 1. The number of cycles to failure at each stress level was found using equation 3. Equation 1 and equation 3 were then combined to form equation 4:

$$D = \sum_{i=1}^k \frac{n_i}{e^{\left(\frac{SI_i - 1}{A}\right)}} \quad (4)$$

A constant scale factor was then applied to each SI as shown:

$$D = \sum_{i=1}^k \frac{n_i}{e^{\left(\frac{SI_i * SF - 1}{A}\right)}} \quad (5)$$

An initial SF was estimated using equation 5 and an initial estimate of the cumulative damage value (D) of one, a standard damage estimate used commonly in practice. This resulted in an initial estimate for SF of 0.515 or 51.5% as shown in Table 2.

Fabrication

A single FRP doubler joint panel was fabricated using the Vacuum Assisted Resin Transfer Molding (VARTM) method. The doubler joint panel was fabricated with nominal dimensions of 36 inches (914 mm) by 45 inches (1143 mm). A total of 22 specimens were obtained from the doubler joint panel for use in both quasi-static and fatigue testing. The fabrication of the doubler plate was consistent with fabrication done in previous research (1), (2).

The base plate of the doubler joint panel consisted of 24 layers of woven roving fabric with a quasi-isotropic pattern $[0/+45/-45/0]_{3sf}$. The base plate was then post-cured for 8 hours at 180°F (82°C). Following post-cure, the top surface of the base plate was sand blasted to provide a better bonding surface for the secondary infusion. Immediately prior to the secondary infusion the top surface of the base plate was cleaned with acetone to prepare the surface for the secondary infusion. The doubler plate followed a similar 24 layer quasi-isotropic pattern as the base plate. The doubler plate geometry is shown in Figure 3. Each successive layer of the doubler plate was cut 0.4 inches (10.2 mm) shorter

than the previous to provide a constant ply drop. The doubler plate was then infused on top of the base plate as shown in Figure 4 and the entire doubler joint panel was post-cured for an additional 16 hours at 180°F (82°C).

After the final post-cure, 22 specimens were cut from the doubler joint panel using a diamond blade wet saw. Specimens were cut at 2 inch (50.8 mm) width. The specimens were then measured and stored in a climate controlled environment at 70°F (21°C) and 50% relative humidity. Four crack gages were applied to each specimen. Each gage was placed such that the edge of the gage was 0.25 inches (6.4 mm) from the start of the first fabric tow running across the specimen as shown in Figure 6. The four crack gages were wired in two series such that the two gages at either end of the specimen were wired together.

Test Setup

Specimens were tested using a 110-kip (500 kN) servo-hydraulic load frame equipped with hydraulic grips. The test setup is shown in Figure 8. Quasi-static tension testing was conducted on four specimens at a load rate of 0.02 in/min (0.51 mm/min). Load, crosshead displacement, and crack gage voltage were collected during static testing at a sample rate of 20Hz. Fatigue testing was conducted in a manner similar to that of the quasi-static testing. In total 16 specimens were tested in fatigue with four different applied scale factors. The maximum and minimum value of the load, crosshead position, and crack gage voltage were recorded at every fourth cycle. Fatigue testing was conducted at a rate of four cycles per second following the random block loading spectra. Failure for both quasi-static and fatigue testing was indicated by a voltage increase in any of the four crack gages. The propagation of the crack through the gage can be seen in Figure 9.

Results

Results from quasi-static testing are shown in Table 3. The load-strain relationship is shown in Figure 11 was assumed to be linear for the purpose of predicting the theoretical fatigue life. It was not necessary to determine a non-linear stress-strain relationship because the theoretical fatigue life was to be verified by testing and the use of a linear prediction tool was sufficient. The average failure load, normalized to width, was 12.4 kips (55.1 kN). The quasi-static test data was used to determine the parameters of the fatigue testing and estimate an initial scale factor as described previously.

In an attempt to validate the initial scale factor and provide a baseline for subsequent tests, two specimens were fatigued at a scale factor of 51.5% as determined from setting D in equation 5 to one and solving

for SF . The two specimens were fatigued at that scale factor for the equivalent of 60 years without failure. The scale factor was then increased arbitrarily to 70% and fatigued using 1-year spectra until failure. The results were used to back-calculate a new estimated scale factor. To do this, the average cyclic peak deformation was determined for each load level. The average was then normalized to width and the average static delamination displacement. The SF for each load level was found by dividing the average normalized peak displacement by the target scale factor. Using equation 1, the cumulative damage was found for each specimen. The calculated damage values for the two specimens were 3.84 and 9.63. Because of the large difference in total damage between the specimens the maximum of the two values was used, the purpose being to provide an upper bound for the scale factor with which to continue testing. A scale factor estimate was found by applying D to equation 5 and solving for another scale factor. By doing this an estimate for the scale factor, to be applied to the first set of fatigue specimens, of 83.8% was found.

The first set of four specimens was fatigued for the complete 30-year loading spectrum at a scale factor of 83.8%. Three of the four specimens tested at this load level reach failure. The crack propagation for one of these specimens after each applied spectrum can be seen in Figure 5, Figure 6, and Figure 7. The scale factor to be applied to the second set of fatigue specimens was then estimated based on the results of the first set of fatigue tests. Similarly, D was back-calculated for each specimen. The average D for the three failed specimens (4.03) was put into equation 5, and the scale factor was estimated at 76.2%. The second set was fatigued at 76.2% and again three of the four specimens achieved failure. The third average D was back-calculated to be 2.75 and the third SF was estimated at 65.8%. The third set of fatigue specimens were tested using this scale factor. None of the specimens tested at a scale factor of 65.8% reached failure. Because of this the scale factor to be applied to the fourth set of fatigue specimens could not be found using test data from the previous set. Instead, the fourth estimate was taken as 71%, halfway between the second and third estimated scale factors. One of the four specimens tested at this scale factor reached failure. Fatigue testing results are shown in Table 4. The variability of the damage value, D , ranged from 57% to 3%, and the variability of the back-calculated theoretical scale factor ranged from 15% to 1%. A curve depicting the theoretical damage as a function of the scale factor is shown in Figure 11.

Conclusions

A test method was adopted to determine an allowable service level load relative to the ultimate strength of an FRP doubler plate joint under variable amplitude fatigue loading spectra. A linear damage

model based on the Palmgren-Miner Rule combined with experimental data was used successfully as a service life prediction tool for a structural FRP component. It was observed that a relatively small increase in the scale factor applied to the loading spectra caused a significant increase in the Miner's Rule damage value.

While this method of testing was successful for application to one particular joint, more work is needed to characterize serviceability issues, specifically in the area of crack propagation. It also may not be practical to apply this type of testing to all possible joint configurations, infusion methods, and materials.

Acknowledgements

Funding for this project was provided by the Office of Naval Research. The authors are thankful to Mr. Brian Jones from the Naval Surface Warfare Center, Carderock Division, for his technical advice and assistance.

References

- 1) El-Chiti F., Lopez-Anido R.A., Landis E., Thibodeau E., and Thompson L. Numerical Approach for Predicting Fracture Failure in Marine Grade FRP Composite Joints. In: SAMPE '08.

- Material and Process Innovations: Changing our World, Long Beach, California, 2008.
- 2) Silva-Muñoz R. and Lopez-Anido R. Monitoring of marine grade composite doubler plate joints using embedded fiber optic strain sensors. *Journal of Advanced Materials*, 2008. 40(4): p. 52-72.
- 3) N.L. Post, J. Cain, K.J. McDonald, S.W. Case, J.J. Lesko, Residual Strength Prediction of Composite Materials: Random Spectrum Loading, *J Engr Frac Mech* vol. 75, pp2707-2724, 2008.
- 4) W.V. Paepegem, J. Degrieck, Effects of Load Sequence and Block Loading on the Fatigue Response of Fiber-Reinforced Composites, *J Mech Adv Mater Struct* vol. 9, pp19-35, 2002.
- 5) M.A. Miner, Cumulative Damage in Fatigue, *J Appl Mech* vol. 67, pp A159-A164, 1945.
- 6) Krueger R., Paris I.L., O'Brien T.K., and Minguet P.J. Fatigue Life Methodology for Bonded Composite Skin/Stringer Configurations. *Journal of Composites Technology and Research* 2002. 24(2): p. 56-79.

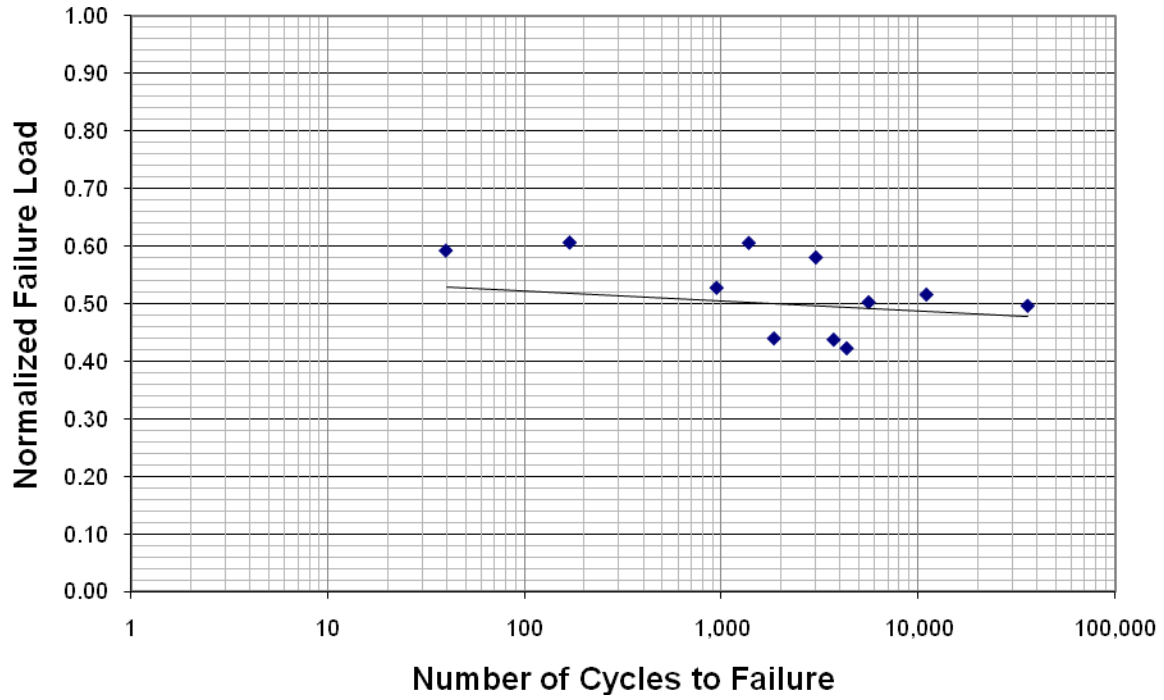


Figure 1: Results of Previous Constant Amplitude Testing

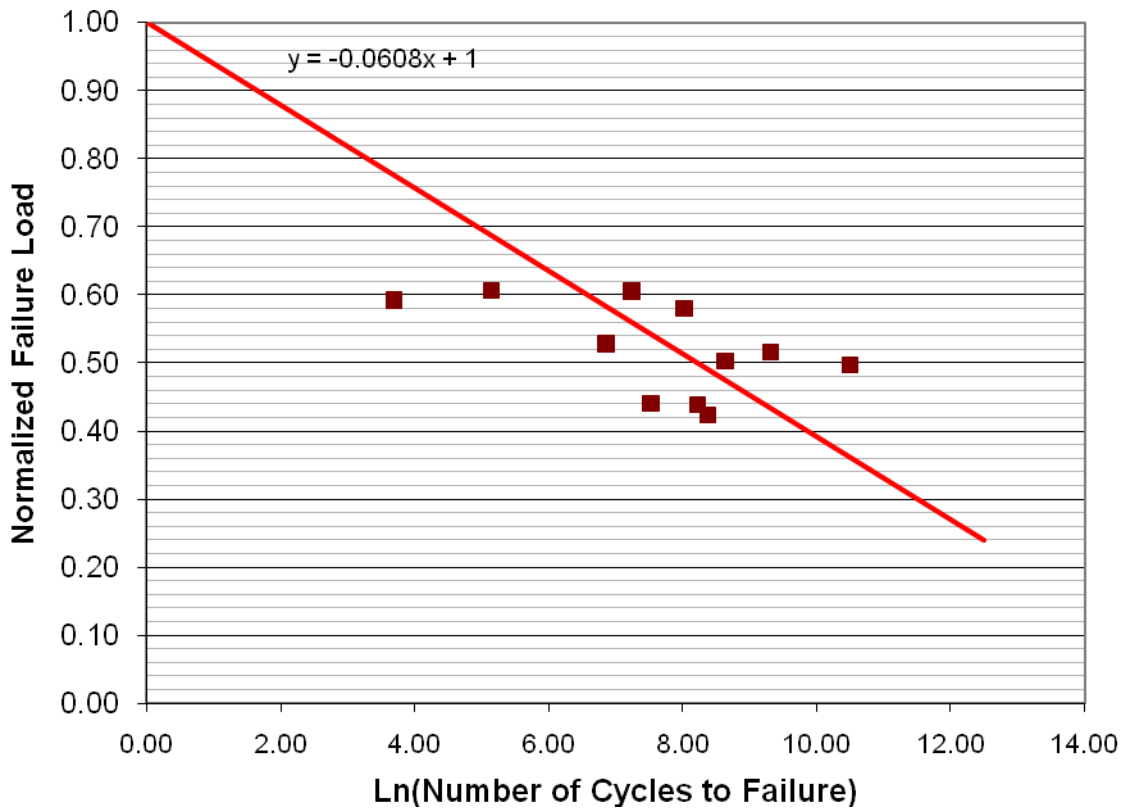


Figure 2: Results of Constant Amplitude Fatigue Testing with Curve Forced Through the Normalized Static Failure Load

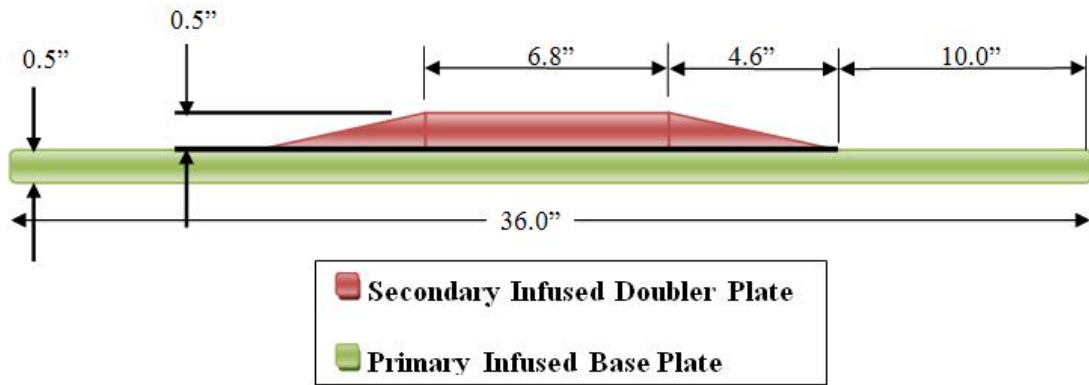


Figure 3: Specimen Geometry



Figure 4: Secondary Infusion of Doubler Plate

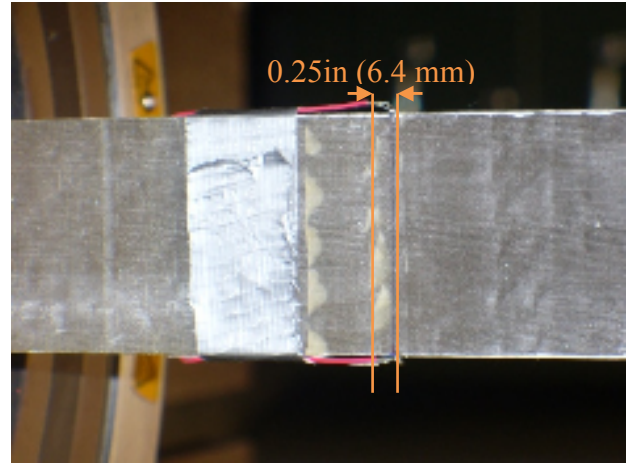


Figure 6: Example Specimen after 5-Year Spectrum Loading

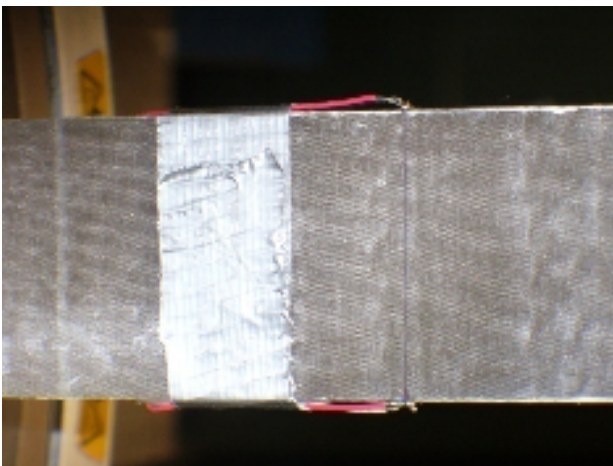


Figure 5: Example Specimen before Testing

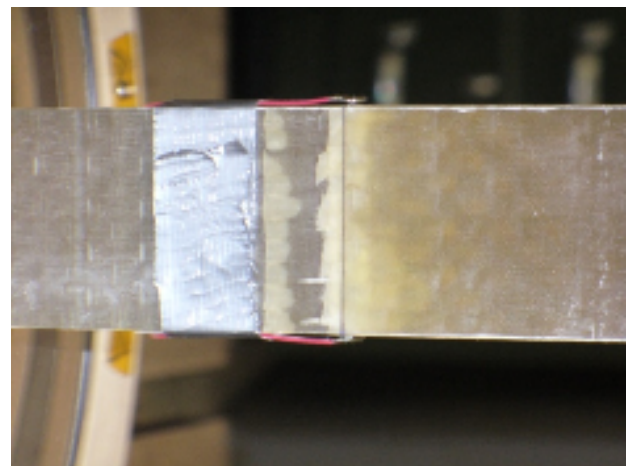


Figure 7: Example Specimen after Full 30-Year Spectra



Figure 8: Testing Setup

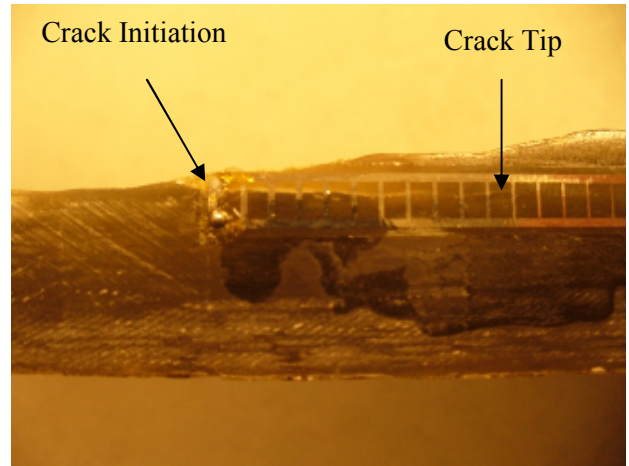


Figure 9: Crack Propagation along Gage Length

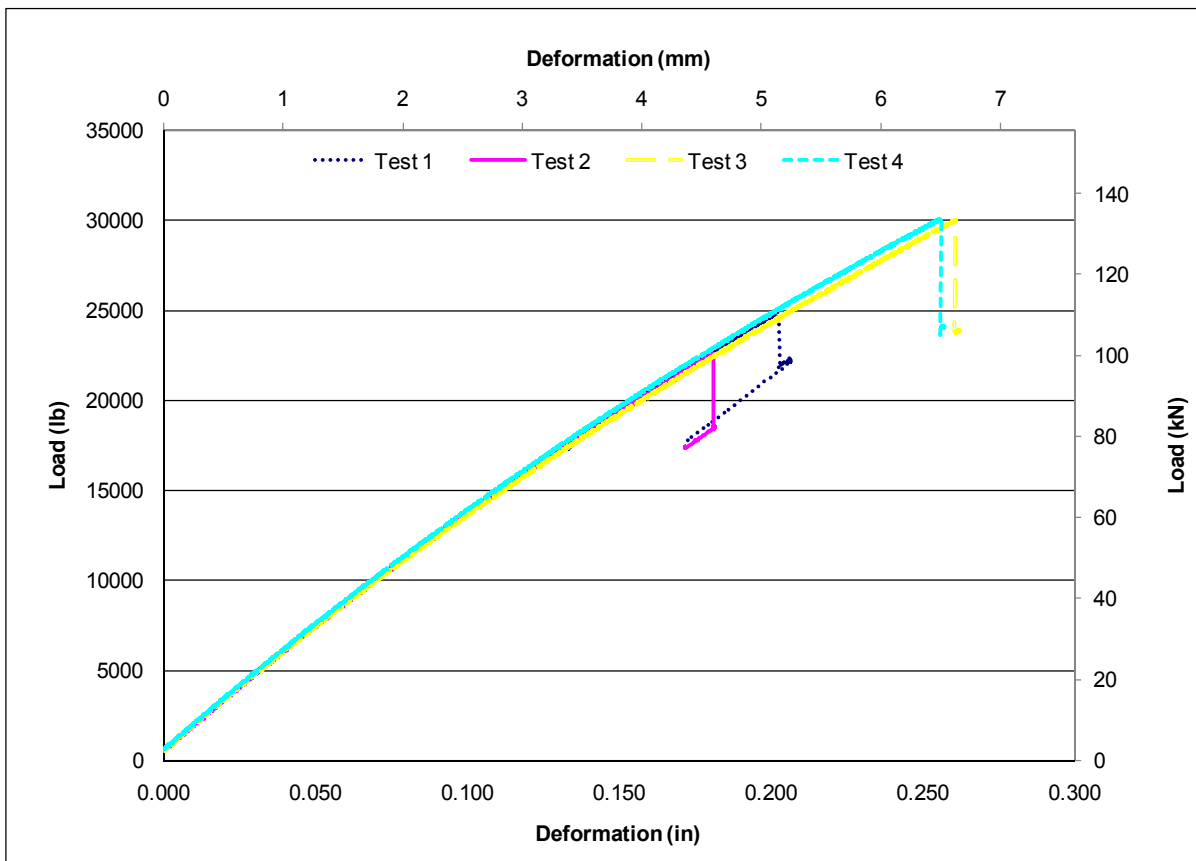


Figure 10: Load-Deformation Relation of Static Specimens

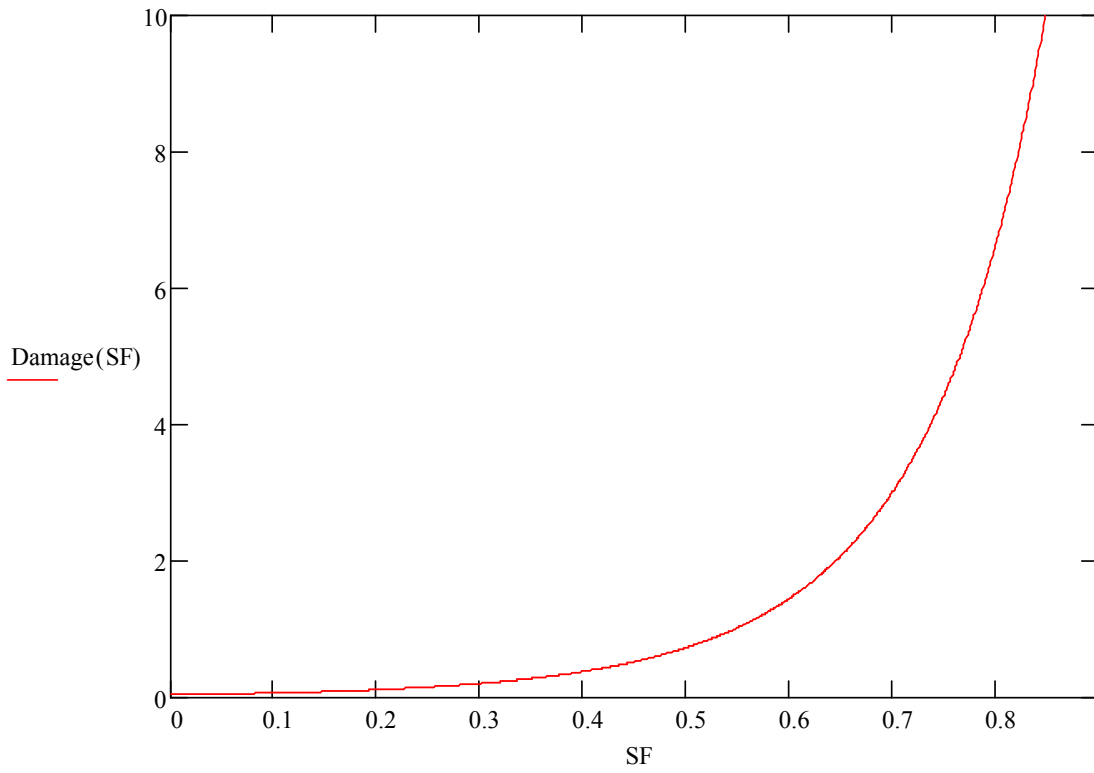


Figure 11: Estimated Damage Curve Based on Scale Factor

Table 1: 5 and 1 Year Fatigue Spectra Stress Indices

Load Step	1 Year Load Sequence		5 Year Load Sequence	
	Cycles	Normalized A	Cycles	Normalized A
1	3044	0.358	15500	0.358
2	1648	0.393	8500	0.393
3	892	0.428	4750	0.428
4	483	0.463	2625	0.463
5	261	0.497	1375	0.497
6	141	0.532	706	0.532
7	76	0.567	382	0.567
8	41	0.602	207	0.602
9	22	0.637	112	0.637
10	12	0.672	60	0.672
11	7	0.707	33	0.707
12	4	0.741	18	0.741
13	2	0.776	10	0.776
14	1	0.811	5	0.811
15	1	0.846	3	0.846
16	1	0.881	2	0.881
17	1	0.846	1	0.916
18	1	0.811	1	1.000
19	2	0.776	1	0.916
20	4	0.741	2	0.881
21	7	0.707	3	0.846
22	12	0.672	5	0.811
23	22	0.637	10	0.776
24	41	0.602	18	0.741
25	76	0.567	33	0.707
26	141	0.532	60	0.672
27	261	0.497	112	0.637
28	483	0.463	207	0.602
29	892	0.428	382	0.567
30	1648	0.393	706	0.532
31	3044	0.358	1375	0.497
32	--	--	2625	0.463
33	--	--	4750	0.428
34	--	--	8500	0.393
35	--	--	15500	0.358

Table 2: Initial Scale Factor Estimate with D Set to One

	Stress Index (SI)	Cycle Count (ni)	Scale Factor (SF): 51.5%	
			Cycles to Failure (Ni)	ni/Ni
S1	0.358	183200	671194	0.273
S2	0.393	99400	499707	0.199
S3	0.428	54100	372034	0.145
S4	0.463	29400	276981	0.106
S5	0.497	15800	206214	0.077
S6	0.532	8462	153527	0.055
S7	0.567	4564	114302	0.040
S8	0.602	2464	85098	0.029
S9	0.637	1324	63356	0.021
S10	0.672	720	47169	0.015
S11	0.707	416	35117	0.012
S12	0.741	236	26145	0.009
S13	0.776	120	19465	0.006
S14	0.811	60	14492	0.004
S15	0.846	56	10789	0.005
S16	0.881	29	8033	0.004
S17	0.916	2	5980	0.000
S18	1.000	1	2929	0.000
Sum(ni/Ni):				1.00

Table 3: Summary of Quasi-static Testing

Normalized to Specimen Width					
Test #	Delamination Disp. in/in (mm/mm)	Initiation Load		Failure Load	
		lb	(kN)	lb	(kN)
1	0.10	12351	(54.94)	12351	(54.94)
2	0.08	9980	(44.39)	9980	(44.39)
3	0.13	14961	(66.55)	14961	(66.55)
4	0.09	11321	(50.36)	12210	(54.31)
Mean	0.0999	12153	54.06	12376	55.05
ST DEV	0.02	2109	9.38	2037	9.06
COV%	22.3%	17.3%		16.5%	

Table 4: Summary of Variable Amplitude Fatigue Testing

Test #	Applied Scale Factor	%	Damage*	Calculated Scale Factor** %	Failure
1	83.8%		3.21	72.7%	Yes
2	83.8%		6.94	83.8%	No
3	83.8%		3.98	75.3%	Yes
4	83.8%		4.91	78.9%	Yes
Avg.	--		4.76	76.8%	--
COV	--		34%	6.3%	--
5	76.2%		2.98	67.3%	Yes
6	76.2%		1.28	56.1%	Yes
7	76.2%		6.24	80.3%	No
8	76.2%		4.01	75.4%	Yes
Avg.	--		3.62	69.8%	--
COV	--		57%	15.2%	--
9	65.8%		1.71	65.0%	No
10	65.8%		1.66	66.2%	No
11	65.8%		1.60	66.3%	No
12	65.8%		1.63	66.3%	No
Avg.	--		1.65	66.0%	--
COV	--		3%	1.0%	--
13	71.0%		4.28	71.4%	No
14	71.0%		4.28	71.4%	No
15	71.0%		4.28	71.3%	No
16	71.0%		2.63	65.2%	Yes
Avg.	--		3.87	69.83%	--
COV	--		21%	4%	--

*Damage value calculated as either theoretical damage at failure or at end of test

**Calculated scale factor is the true applied scale factor for unfailed specimens or the theoretical 30-year scale factor for failed specimens